Satellite-Image-Derived Velocity Field of an Antarctic Ice Stream

R. A. BINDSCHADLER AND T. A. SCAMBOS

The surface velocity of a rapidly moving ice stream has been determined to high accuracy and spatial density with the use of sequential satellite imagery. Variations of ice velocity are spatially related to surface undulations, and transverse velocity variations of up to 30 percent occur. Such large variations negate the concept of plug flow and call into question earlier mass-balance calculations for this and other ice streams where sparse velocity data were used. The coregistration of images with the use of the topographic undulations of the ice stream and the measurement of feature displacement with cross-correlation of image windows provide significant improvements in the use of satellite imagery for ice-flow determination.

TWO URGENT ISSUES BEING ADDRESSED BY ANTARCTIC glaciologists are the mass balance of the Antarctic ice sheet and the ice sheet's future behavior. Mass balance refers to the rate at which the volume of the ice sheet is changing; it depends on the balance between snow accumulated on the ice sheet and ice discharged from it. Predictions of the future of the ice sheet depend on the ability to predict changes in snowfall and ice discharge. Changes in ice sheet volume are directly connected to changes in global sea level.

Addressing these issues requires glaciologists to monitor and understand the motion of the large ice streams that drain much of Antarctica. Typical ice streams are hundreds of kilometers long, tens of kilometers wide, and move at speeds of hundreds of meters per year. Although these rapidly moving conveyors of ice are major components of the dynamics of the ice sheets, few data are available on their extents and velocities. Ice streams are fed by ice collected in their catchment basins within the ice sheet. In individual ice stream basins, detailed measurements have often revealed sizable mass imbalances, and large differences in mass balance can occur between adjacent basins (*1*). The rapid time scale over which the discharge can change is indicated by field measurements of the downstream end of a major ice stream in West Antarctica; this stream decelerated by 20 percent in an 11-year period (*2*). Because the Antarctic ice sheet comprises a large number of basins, more data are needed to assess the mass balance of each basin and how this balance may be changing. Before this is done, any estimate of the total mass balance of Antarctica must be considered tentative (*3*).

R. A. Bindschadler is with the National Aeronautics and Space Administration, Goddard Space Flight Center, Code 971, Greenbelt, MD 20771. T. A. Scambos is with ST Systems Corporation, 4400 Forbes Boulevard, Lanham, MD 20706.

In this article we describe a technique of measuring ice-stream velocity at large scales in areas of 100 percent snow cover from satellite imagery. The development of this method is important because its application will enable the velocities of many ice streams to be determined more rapidly, less expensively, and more safely than with currently employed techniques. We have applied this method to ice stream E to investigate the nature of ice-stream flow and evaluate its mass balance.

Methods for ice velocity measurement. Numerous techniques have been used to measure the velocity of flowing ice. All methods involve determining the position of markers at two times. When solid rock is visible from the ice surface, conventional surveying methods can be used (*4*). In order to obtain denser coverage, photogrammetric methods have been applied to aerial photographs or high-resolution satellite imagery. However, these methods have been limited to areas where well-defined, fixed points are plentiful enough that multiple photographs or images can be coregistered (*5*).

Most of the ice sheet, however, is devoid of suitable fixed points. In these areas, techniques based on satellite positioning systems have been the only method for measuring ice motion. Position data are needed for either a photogrammetric ground-control net (*6*) or for isolated measurements of velocity (*7*). In both cases, the disadvantage is the costly logistical support required to put observers in the field.

We have developed a cross-correlation method for measuring ice stream motion with sequential satellite imagery that requires no surface field team. The topographic undulations of the ice stream itself are used for coregistration. Because all ice streams appear to have suitable undulations, we believe this technique can be applied to high-resolution image data of any ice stream.

We have applied our method to two Landsat Thematic Mapper (TM) images of ice stream E, West Antarctica (see Fig. 1). The images (ID 510511451 and ID 423411503; both Path 7 Row 119) were acquired nearly 2 years apart (16 January 1987 and 12 December 1988). Quadrant 1 of both scenes covers an area extending across most of ice stream E and includes a portion of the ridge between ice streams D and E (Fig. 2) The banded, crevassed, and strongly undulated surface of the ice stream contrasts markedly with the smoother ice of the ridge. Flowbands on the ice stream indicate the history of flow direction. Undulations on the ice stream are more prominent than on the ridge, but their distribution is not uniform. There is a long series of undulations running at a 45° angle across the center of Fig. 2, whereas near the left edge of the figure there is a 5-km-wide band running the length of the image in which no undulations appear.

Coregistration of the images was based on the assumption that surface undulations on fast moving ice are spatially related to

subglacial topography and, therefore, are fixed in space. Because the albedo of the surface snow is nearly constant for visible and near-infrared wavelengths, brightness variations in the image correspond to the surface topography (*8*). The influence of subglacial roughness on surface topography increases with the ice velocity (*9*).

We coregistered the images by matching the positions of the larger, low-amplitude surface features occurring in each image. To enhance the topographic features in the images and reduce the noise inherent in any single band, we used the first principal component (PC1) of TM bands 2, 3, 4, and 5 and removed scan-line striping from the PC1 image with a simple algorithm (*10*). The PC1 images were then filtered with a low-pass spatial frequency filter with a cutoff wavelength of 1 km to remove small, sharp topographic features such as crevasses and snow mounds that move with the surface ice and interfere in the coregistration process. By flickering the two filtered images on a computer display, we were able to detect an offset in the undulation field. The optimal coregistration was determined by shifting the relative positions of the images until no offset was detectable. We were able to coregister the images within one image pixel (28.5 m) after only a few iterations (*11*). Differences in sun elevation or azimuth from one image to another can alter the appearance of the low-relief undulation field and interfere in the coregistration process and thus result in a systematic error in the derived velocities. However, the apparent displacement of undulations caused by possible differences in sun elevation is typically less than a single pixel. Image distortion would cause a nonsystematic error, but, for modern image systems, this is less than a single pixel anywhere within the image. Nevertheless, to minimize such effects, it is most desirable to use image pairs taken as close as possible to the same calendar date and time.

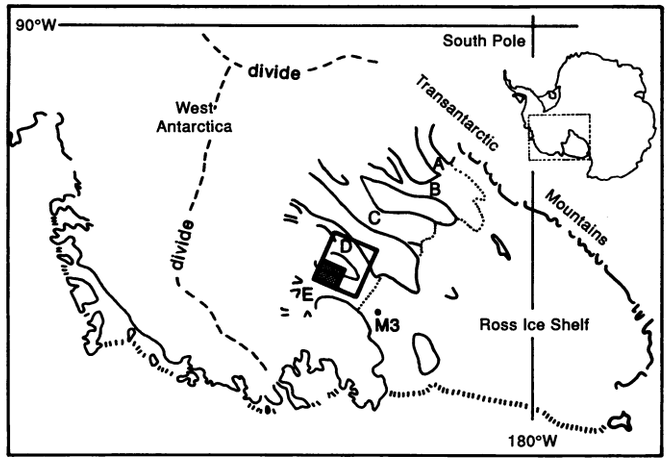

Fig. 1. Map of Antarctica identifying major ice streams (A to E), RIGGS station M3, and the location of Landsat images used in this study. Heavy outline is full Landsat scene; Quadrant 1 is shaded.

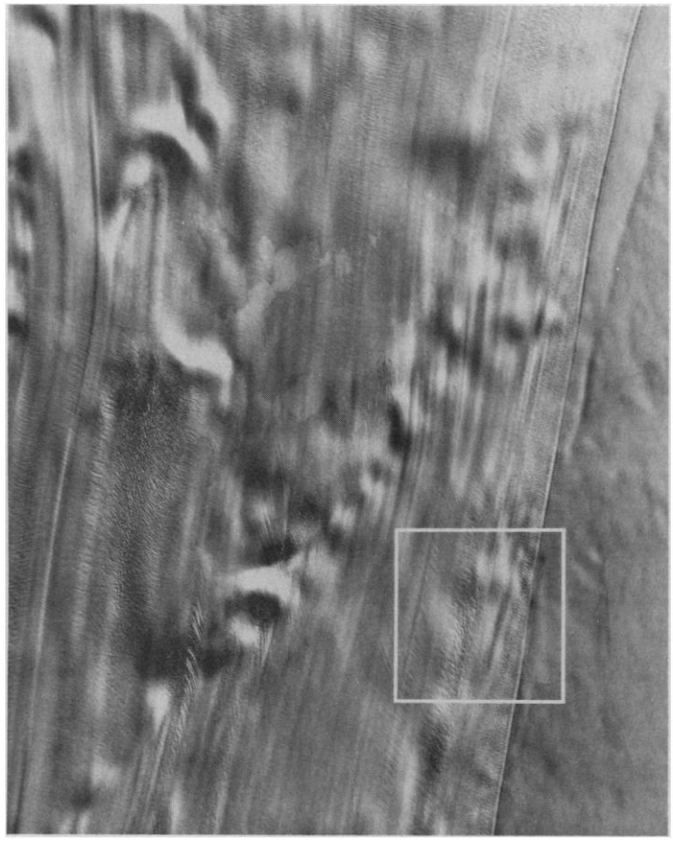

Fig. 2. First principal component (PC1) composite of Quadrant 1 image of ice stream E taken on 16 January 1987. Sun position is at an azimuth of 105° and an elevation of 18°. Outlined area is location of subscene shown in Fig. 3.

The coregistration of the two images was performed independently for five different subscenes within the area common to both images. The mean offset to achieve coregistration was +22 line pixels and −71 sample pixels (corresponding to the direction of satellite motion and the direction transverse to satellite motion, respectively), and no rotation was required. The offsets for all five subscenes agreed to within one pixel. Such a small offset reduced the effect of possible distortions in the 7.5° field of view of the TM sensor. The absence of rotation eliminated possible errors of position determination that would have been caused by resampling.

The constancy of the offset vector across the entire image established that the undulation field was either fixed or moving at constant speed. Compelling evidence that the undulation field was fixed comes from additional coregistered subscenes in Quadrant 2 of the TM images. Although these subscenes were of ice stream D (see Fig. 1), they required an almost identical offset correction for coregistration. Thus, if the undulations were moving, they were moving at nearly identical speeds in nearly identical directions on two different ice streams, which themselves were moving at different speeds and in different directions. This condition is highly improbable.

Once the appropriate coregistration offset was determined, we applied it to high-pass spatially filtered versions of the PC1 images. As with the low-pass filter, a cutoff wavelength of 1 km was used. High-pass filtering removed the long-wavelength undulations from the images and enhanced small surface features such as crevasses and snow dunes. Displacements in these features between the two images, divided by the time interval separating the two images yields the ice surface velocity relative to the undulation field.

In the point-picking method of determining velocities from sequential imagery, the displacements of sharp or distinct features are measured by locating them on each image. Preferred features are those that can be resolved and located with an accuracy of less than one image pixel. In our initial analysis of the coregistered imagery we used this method and determined velocities at 248 points distributed throughout the image area. There were many more features that could have been measured. In consideration of the position uncertainty of plus or minus one pixel (28.5 m) and the temporal separation between the two images, the random error in velocity measurement with this method is ±20 m per year; there is also a possible systematic error in any subscene of ±20 m per year

associated with the coregistration (*12*). In addition, sharp features do not occur in some areas, and less suitable features were used. In such areas, location errors are expected to be somewhat larger.

In the cross-correlation method, a computer algorithm was used that takes a small image area (or "window") containing distinct features in the first image and searches a user-specified region in the second image for the area (or "target window") that best matches the pattern of brightness values in the original area. For each target window the residual between the brightness values in the target window and the original window is calculated. Thus, a residual is calculated at each pixel within the search area; the location of the minimal residual gives the best estimate of the displacement of the features in the original window from the first image to the second image. Along with the position of the minimum, the program calculates an uncertainty in this position. If the uncertainty exceeds a user-specified threshold, no displacement is calculated.

The cross-correlation technique offers two important advantages. First, it allows reliable ice velocity measurements by use of diffuse or subtle surface features such as crevasse scars and broad dunes or pits that lack sharp boundaries. This advantage significantly expands the regions of ice sheet over which surface velocities can be determined because there are broad regions of ice streams and ice sheets where such subtle features are seen but sharper features are entirely absent. The second major advantage is that it permits displacements to be measured to better than one-pixel accuracy. This accuracy is achieved by determination of the position of the residual minimum in the search region by interpolation of residual values between pixel locations.

We tested the cross-correlation method by comparing velocities determined by this method with the velocities already determined by the point-picking method. A window with dimensions of 32 by 32 pixels was centered on each of the 248 points, and a corresponding search region with dimensions of 64 by 64 pixels was positioned in the second image on the basis of the velocities determined from the first method. The search regions were large enough that the two methods were independent. In 196 cases, the new method was successful in providing a velocity to subpixel resolution. We reviewed individual cases of subpixel-level displacements to confirm that the fractional displacements calculated by the program were correct (*13*). Thus, the velocities calculated by the cross-correlation method are more accurate than velocities calculated by the point-picking method.

Most failures in the cross-correlation method occurred within the shear margin at the edge of the ice stream. Shearing causes distortion in the spatial pattern of features. Reducing the size of the window or altering its shape to conform to the anticipated distortion could reduce the chance for failure of the cross-correlation method. For example, a window that was narrow in the direction across the flow but longer in the direction of flow would be expected to improve the algorithm's ability to find a reliable residual minimum. The cross-correlation method also failed in areas where only a single faint feature was present or where clouds partly obscured features of the ice stream in one of the images.

An image subscene of the southern shear margin of the ice stream illustrates the method comparison (Fig. 3). As a result of the subpixel location capability of the cross-correlation method, the estimated errors of velocity calculated by this method are dramatically lower than for the velocities determined from the point-picking method. The standard error of velocities from the cross-correlation method in this area is ±2.3 m per year, versus ±20 m per year for the traditionally determined velocities. Even more dramatic is the greater consistency in flow direction; the flow direction is expected to be uniform. The standard error in the flow direction for the subscene is ±9° as determined by the point-picking but only ±0.5° for the cross-correlation analysis.

Velocity structure of Ice Stream E. The average velocity of ice stream E over the study region is approximately 360 m/year, but the pattern of velocity shows several large-scale structures (Figs. 4 and 5) (*14*). Although the largest gradient in velocity (and thus strain rate) occurs along the ice-stream margin, two other regions show evidence of high strain rates. One is located near the left edge of the map scene, and the other is located just below the center of the map where the velocity is at a local minimum of 308 m per year and a maximum of 464 m per year. The nearest field-measured velocity with which to compare our data was determined 200 km downstream at RIGGS stations M3 on the Ross Ice Shelf in the mouth of ice stream E (*15*) (see Fig. 1). The velocity determined at this location, 414 m per year, is consistent with out measurements.

The high velocity gradient measured at the margin of ice stream E is characteristic of ice streams and represents a band of intense shear. The magnitude of this transverse velocity gradient is roughly 0.08 per year; exceeding the critical strain rate required for crevasse initiation (*16*). On nearby ice stream B (see Fig. 1), where velocity gradients were measured by optical survey methods, the band of intense shear is almost twice as wide as on ice stream E (Fig. 6) (*17*). The reported observation that the shear band of ice stream B is a continuously crevassed surface whereas the margin of ice stream E appears much narrower has led to the inference that the shear margin of ice stream E might be much narrower than our measurements indicate (*18*). Whether there is any significance to the differences in margin widths of ice streams B and E is not known at this time. One possibility is that a narrower margin represents a more stable margin as shear becomes concentrated in an ever-decreasing band of intense deformation.

The local minimum of velocity in the part of the ice stream analyzed occurs more than 20 km from the margin. The velocity

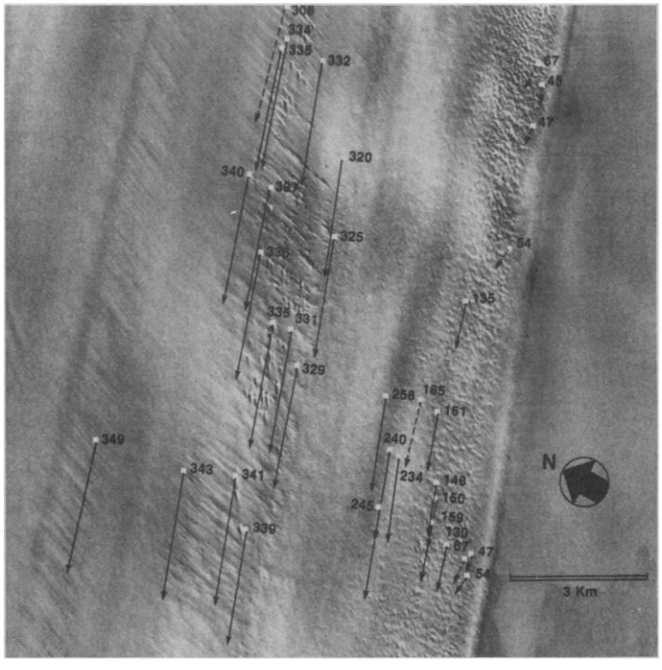

Fig. 3. Ice velocities (in meters per year) measured near the margin of ice stream E (see Fig. 2 for scene location). The motion of features marked by white squares are measured by both the cross-correlation method and the point-picking method. Solid vectors indicate the velocity determined from the cross-correlation method; dashed vectors indicate the velocity determined from the point-picking method when the cross-correlation analysis failed.

pattern shows that this minimum is associated with a widespread area of deceleration and with the set of undulations striking obliquely across the ice stream (Fig. 5). The southward deviation of the flowbands as they approach these undulations provides further evidence that these undulations exert a major influence on the flow of the ice stream. In the absence of ice-thickness data, we infer that these features are caused by a large subglacial ridge overridden by the ice stream. If this is the case, this ridge presents a major source of resistance to the flow of the ice stream.

A narrow channel in the ice stream, marked by prominent flowbands, winds along the leftmost part of the image and avoids both the oblique set of undulations as well as other isolated undulations. Ice in this channel accelerates for 70 km along the entire length of the study area. Midway over this distance a strong velocity gradient occurs; the position of this gradient corresponds to the region where transverse crevasses are generated. The longitudinal strain rate in this section is roughly 0.014 per year, more than sufficient for initiation of crevasses. The downstream persistence of this crevasse field is attributed to the continued acceleration of the ice in this channel.

The sustained acceleration is probably the result of a gradual thinning of the ice stream as it approaches the Ross Ice Shelf (*19*) and the narrowing of the ice stream (see Fig. 1), but it may also be the result of variations in subglacial conditions that are known to strongly influence the nature of ice-stream flow, such as bed composition and subglacial water pressure (*20*). Downstream of our measurement area, the width of the ice stream begins to increase. At the position of RIGGS station M3 (Fig. 1), vertical thinning and transverse widening have roughly equal, but opposite, effects on the velocity.

Adjacent to the transverse crevasses is a broad region of crevasses with orientations that suggest that they were initiated by shear with faster flow to the left. Again the velocity contours are consistent with this pattern, and the image shows that the lower velocities are spatially related to the large undulation just upstream of these shear crevasses. Shear crevasses are formed in similar situations farther downstream where areas of local shear are generated as the ice passes over the oblique set of undulations. In all cases, the pattern of the freshly formed crevasses conforms to the derived pattern of velocity.

Implications for mass balance calculations of ice streams. The velocity data from ice stream E obviously do not fit the plug-flow model where velocity is assumed to be constant across the width of the ice stream

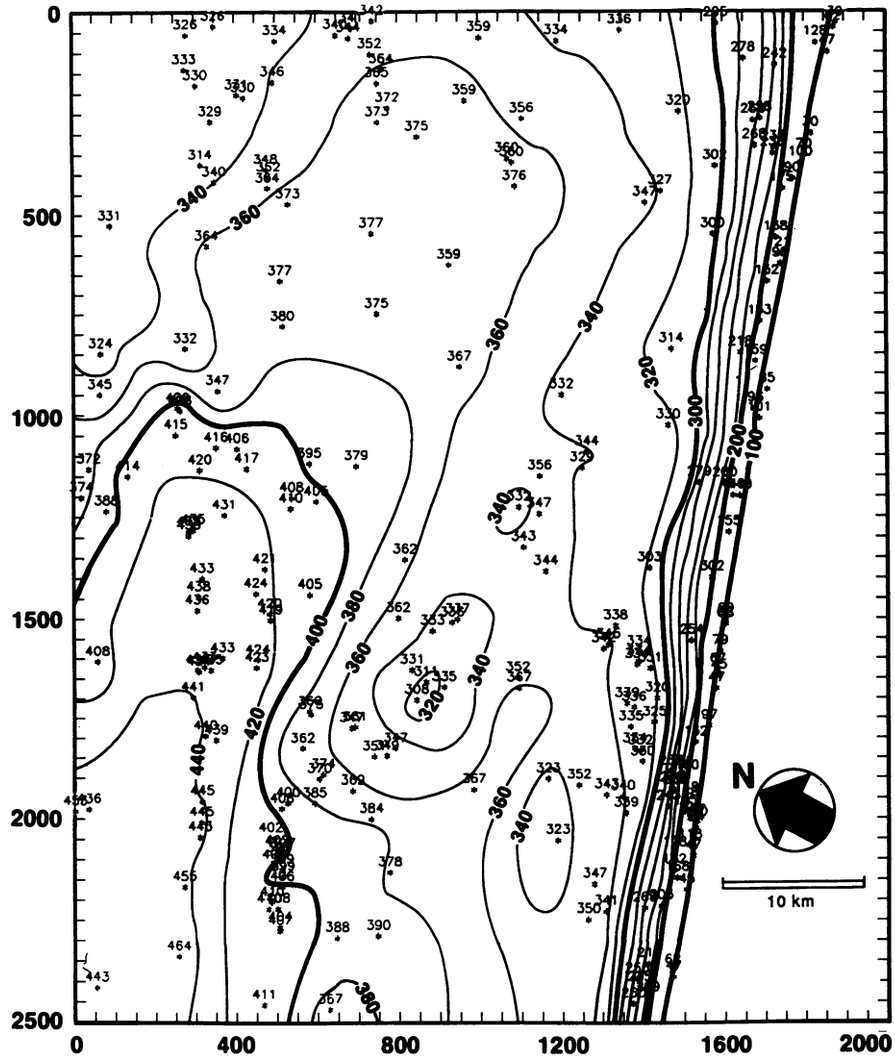

Fig. 4 (above). Velocity map of area covered in Fig. 2. Contours at an interval of 20 m per year were generated initially by computer software and modified by hand. Coordinates are pixel numbers. Pixel dimensions are 28.5 by 28.5 m.

Fig. 5 (right). Velocity contours from Fig. 4 superimposed on image (Fig. 2).

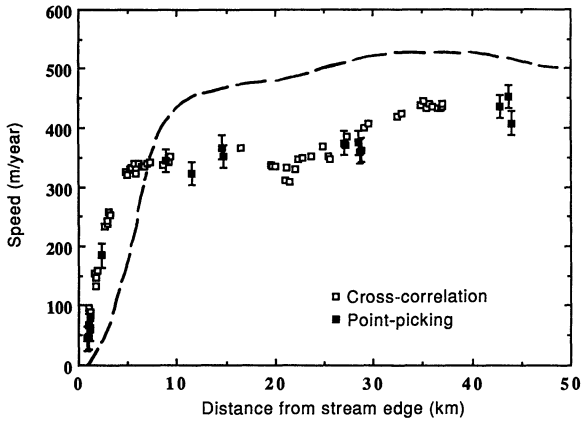

Fig. 6. Transverse velocity profile across ice stream E. Vertical bars indicate estimated random error (1 SD) determined by the point-picking method. Errors for velocities determined by the cross-correlation method (open squares) are smaller than the symbol size. Dashed line is transverse profile from ice stream B (*17*).

(with the exception of relatively narrow shear margins). Our data indicate that in our study area transverse variations in velocity can be as large as 30 percent (Fig. 6). Other ice streams, such as ice stream B, which are heavily crevassed probably exhibit similar velocity variations. In these cases, isolated measurements of velocity provide an inadequate estimate of mean velocity and ice discharge rates. Thus, the velocity interpolations across crevassed areas made by Shabtaie *et al.* (*21*) as part of their calculation of the local pattern of mass balance of ice stream B may contain errors larger than they estimated. In addition, velocities that have been measured by field parties usually are collected in crevasse-free areas. These measurements are prone to avoid areas where the higher gradients in the velocity field occur and to miss velocity variations that are important in understanding the dynamics of ice-stream motion.

The mass balance of ice stream E has been estimated to be slightly negative (-3.9 ± 5.1 km^3 per year) (*22*) on the basis of the single velocity measurement at RIGGS station M3 downstream of the ice stream and an estimate of the rate at which snow accumulated over the entire catchment basin of the ice stream. Another analysis of the accumulation was completed as part of a modeling study of the behavior of ice stream E (*23*). This model included a hypothetical profile of the steady-state velocity along the entire ice stream. In the region of our measurements, the steady-state, or balance velocity was calculated to be no more than 250 m per year. Our measurements indicate that the actual average surface velocity is approximately 350 m per year. Because of the nature of ice-stream motion, this velocity probably does not change with depth. Thus, our data support the earlier contention that ice stream E is in negative mass balance but indicate that the imbalance at this point of the ice stream is -8.3 km^3 per year; substantially higher than previously estimated (*24*). More detailed measurements of the velocity field are needed in conjunction with ice thickness measurements to produce a better estimate of the mass balance pattern.

The ability to coregister satellite imagery of ice streams in areas lacking fixed rock outcrops greatly extends the utility of these data in glaciological research. The addition of our cross-correlation method for more accurate velocity determinations and determinations of features heretofore too subtle or diffuse to resolve means that glaciologists no longer need to work with sparse data sets of surface velocity. Removal of these two constraints paves the way for the collection of much needed surface velocity data to better assess the current mass balance of the ice sheets and whether that mass balance is changing. In addition, these data should permit more quantitative studies of the dynamics of ice-stream motion and assist in siting of surface-based investigations such as ice drilling to directly sample the subglacial bed. In regions where characteristic features are abundant, it is expected that velocity fields can be measured with sufficient accuracy to permit the calculation of strain fields and, from them, complete force-balance studies that are needed to quantify the dynamic behavior of the ice stream.

REFERENCES AND NOTES

1. I. M. Whillans and R. A. Bindschadler, *Ann. Glaciol.* **11**, 187 (1988); S. Shabtaie, C. R. Bentley, R. A. Bindschadler, D. R. MacAyeal, *ibid.*, p. 137.
2. S. N. Stephenson and R. A. Bindschadler, *Nature* **334**, 695 (1988).
3. For example, C. R. Bentley, *Eos* **70**, 1002 (1989).
4. For example, R. A. Bindschadler, W. D. Harrison, C. F. Raymond, R. S. Crosson, *J. Glaciol.* **18**, 181 (1977).
5. H. H. Brecher, *Ann. Glaciol.* **8**, 22, (1986); B. K. Lucchitta and H. M. Ferguson, *Science* **234**, 1105 (1986).
6. M. Jackson and I. M. Whillans, *Eos* **69**, 365 (1988).
7. J. McDonald and I. M. Whillans, *Ann. Glaciol.* **11**, 83 (1988).
8. J. A. Dowdeswell and N. F. McIntyre, *J. Glaciol.* **33**, 16 (1987).
9. I. M. Whillans and S. J. Johnson, *ibid.* **29**, 78 (1983).
10. In the principal component analysis, linear combinations of the original data bands are searched for that maximize the variance of the data in a minimum number of components. Thus, the first principal component contains the greatest variance. O. Orheim and B. K. Lucchitta [*Ann. Glaciol.* **11**, 109 (1988)] have shown that the first principal component produces a clearer image of ice sheet topography. Scan-line filtering method is reported by *Photogram. Engr. Remt. Sens.* **55**, 327 (1989).
11. In principle, the cross-correlation method used to determine feature displacement could be used to provide subpixel coregistration, however, the maximum window size permitted by the cross-correlation software we used was too small to permit it being used in this way.
12. Limits for random errors are reported as ± 1 SD.
13. The two images were aligned to the nearest integral number of pixels on either side of the program-determined value. For example, if the program determined a displacement of 25.7 pixels, the first image was shifted relative to the second by both 25 and 26 pixels. In both shifts the features in the two images did not match precisely, but an estimate of the relative mismatch for each shift provided a rough estimate of the appropriate subpixel displacement.
14. Gridding and contouring were performed on a desktop computer with the use of commercial software based on kriging principles. Final contours were produced by hand smoothing and correcting obvious artifacts of the computer-generated contours.
15. R. H. Thomas, D. R. MacAyeal, D. H. Eilers, D. H. Gaylord, *Antarct. Res. Ser.* **42**, 21 (1984).
16. G. Holdsworth, *J. Glaciol.* **8**, 107 (1969); P. L. Vornberger and I. M. Whillans, *ibid.* **36**, 3 (1990).
17. R. A. Bindschadler, D. R. MacAyeal, S. N. Stephenson, *J. Geophys. Res.* **92**, 8885, (1987). See figure 103 in C. Swithinbank, *U.S. Geol. Surv. Prof. Pap. 1386-B* (1988) for a photograph of the northern margin of ice stream B.
18. S. N. Stephenson and R. A. Bindschadler, *Ann. Glaciol.* **14**, 273 (1990).
19. D. Drewry, *Antarctica: Glaciological and Geophysical Folio* (Scott Polar Research Institute, Cambridge, 1983).
20. H. Englehardt, N. Humphrey, B. Kamb, M. Fahnestock, *Science* **248**, 57 (1990).
21. S. Shabtaie, C. R. Bentley, R. A. Bindschadler, D. R. MacAyeal, *Ann. Glaciol.* **11**, 137 (1988).
22. S. Shabtaie and C. R. Bentley, *J. Geophys. Res.* **92**, 1311 (1987).
23. C. S. Lingle, *ibid.* **89**, 3523 (1984).
24. In this calculation we assume that the imbalance in velocity is 100 m per year and use values from Lingle (*23*) of 1100 m for the average depth and 75 km for the width.
25. We thank the U.S. Geological Survey who shared the cost of these images as part of a joint project focusing on the Siple Coast region. We also acknowledge the able assistance of N. Gilra in determining pixel locations and of M. Dutkiewicz and J. Wilson in testing the computer method. The research was supported by funds from the National Science Foundation under grant DPP-8614407.

6 December 1990; accepted 25 February 1991